J Ambient Intell Human Comput (2019) 10:89–106
DOI 10.1007/s12652-017-0606-1

ORIGINAL RESEARCH

Online human movement classification using wrist-worn wireless sensors

Peter Sarcevic[1] · **Zoltan Kincses**[2] · **Szilveszter Pletl**[2]

Received: 8 February 2017 / Accepted: 15 October 2017 / Published online: 26 October 2017

Abstract The monitoring and analysis of human motion can provide valuable information for various applications. This work gives a comprehensive overview about existing methods, and a prototype system is also presented, capable of detecting different human arm and body movements using wrist-mounted wireless sensors. The wireless units are equipped with three tri-axial sensors, an accelerometer, a gyroscope, and a magnetometer. Data acquisition was done for multiple activities with the help of the used prototype system. A new online classification algorithm was developed, which enables easy implementation on the used hardware. To explore the optimal configuration, multiple datasets were tested using different feature extraction approaches, sampling frequencies, processing window widths, and used sensor combinations. The applied datasets were constructed using data collected with the help of multiple subjects. Results show that nearly 100% recognition rate can be achieved on training data, while almost 90% can be reached on validation data, which were not utilized during the training of the classifiers. This shows high correlation in the movements of different persons, since the training and validation datasets were constructed of data from different subjects.

Keywords Activity recognition · Wearable sensors · Feature extraction · Time-domain analysis · Dimension reduction

1 Introduction

The analysis and real-time monitoring of human body motion is a widely-studied field of industrial, entertainment, health, and medical applications (Cornacchia et al. 2017). Such systems can be used for robot control, human–computer interaction, assisted living, gaming, fall detection, epileptic seizure detection, telerehabilitation, analysis of daily activities, emergency detection, health monitoring, or even human worker activity recognition in industrial environments.

Human motion can be split into two basic categories, activities and movements. Movements typically last for several milliseconds or seconds, while an activity comprises of different movements, and can last for even minutes or hours (Varkey et al. 2012). For example, a "walking" activity contains several short physical leg movements. But more complex activities can also be defined, such as "cooking", which is composed of multiple shorter activities in a specific sequence, like "walking", "arm raising", "standing", etc.

Sensor-based motion recognition integrates the emerging area of sensor networks with machine learning techniques. Inertial and magnetic sensors are widely used in wearable devices for motion recognition, due to their small size, low cost, and small energy consumption. These wearable devices applied to human bodies form Wireless Body Sensor Networks (WBSNs) (Alemdar and Ersoy 2010). Another option for human motion monitoring can be the use of Personal Area Networks (PANs), which are composed of environmental sensors, like Radio-Frequency Identification (RFID)

✉ Peter Sarcevic
sarcevic@mk.u-szeged.hu

[1] Technical Department, Faculty of Engineering, University of Szeged, Moszkvai krt. 9, 6725 Szeged, Hungary

[2] Department of Technical Informatics, Faculty of Science and Informatics, University of Szeged, Arpad ter 2, 6720 Szeged, Hungary

readers, video cameras, or sound, pressure, temperature, luminosity, and humidity sensors. The vision-based activity recognition systems are the most popular types of PANs. One of the main advantages of body sensor networks to systems using cameras with fix places is that they support persistent monitoring of a subject during daily activities both in indoor and outdoor environments. The vision-based systems are also influenced by environmental factors, such as lighting conditions, and they incur a significant amount of computational cost.

Due to the difficult implementation of signal processing algorithms on resource constrained wireless nodes, the design of WBSN-based applications is a very complex task (Aiello et al. 2011; Gravina et al. 2017). Efficient implementation of WBSN applications requires appropriate usage of energy, memory, and processing. These systems must meet computational and storage requirements. They should also be wearable, which affects the possible usable battery size and therefore its duration. This is a challenging task, because these applications usually require high sampling rates of the sensors, real-time data processing, and high transmission capabilities.

The goal of this research was to develop a wearable wireless system which does not disturb the user in free movement, and which can efficiently recognize basic body and arm movements using an online classification algorithm. It was also important to explore different setups to minimize the cost, the energy consumption, and the memory requirements, besides maximizing the classification efficiency.

In the study, a prototype system is proposed which uses 9DoF sensor boards mounted on Wireless Sensor Network (WSN) motes, which were attached to the wrists of the subjects. The developed system was used to record measurements for multiple activities. The proposed system does not require any additional server for the processing of the data, and it is also suitable for the logging of the activities.

Related works (described in Sect. 2) mainly do not deal with the implementability of the algorithms on the used hardware, or use a centralized server to do the necessary computation. The use of processing servers can cause several disadvantages. First, the communication in the network is very costly due to the high sampling frequencies of the sensors, and secondly, since the subjects are moving, they can get out of the range of the server if its place is fixed. Some works implement their algorithm on a smartphone, but the performance of these systems can be affected by the varying placement of the units, or their use during the operation of the algorithm. Based on the above considerations, it was reasonable to develop an online method, and to examine the hardware implementability of different classification algorithms. Linear discriminant analysis (LDA)-based dimension reduction was also tested to investigate its effect on the tested classification methods in the meaning of recognition efficiency, memory consumption, and training time.

Since related studies mainly consider complex activities or use more than 1–2 s of data for classification of motions, it was necessary to investigate the barriers in the performance when decreasing the processing window width. Related works which utilize multiple sensor types also do not consider the effect of different sensor types on classification efficiency. To find the optimal setup, multiple classification methods were investigated for various datasets, which were generated based on different sampling frequencies, processing window widths, feature extraction modes, and used sensor types. The extraction and reduction of feature vectors were also tested in multiple ways. The features were computed utilizing the sensor axes separately and using the magnitude. To reduce the required computation, only time-domain analysis was performed during feature extraction. An aggregation-based feature reduction method is also proposed in this study, which can help the system to be less sensitive to differences in orientations of the sensors on the arms.

In this study, the data from the two wrists are used together for classification. An initial investigation was presented previously (Sarcevic et al. 2015a). A hierarchical-distributed approach was also tested with the collected data (Sarcevic et al. 2015b), where the movement class was determined for each arm separately, and one of the units combined the two classes to get the movement type of the entire body and arms. The approach reduces the energy consumption, since it needs less communication between the units, but the results showed that the recognition efficiency is lower than when data from the two sensor boards are used together in the classification process.

The rest of the paper is organized as follows. Section 2 introduces related work, Sect. 3 presents the prototype measurement system, the defined activities, and the data acquisition. The proposed classification algorithm, including the used time-domain features (TDFs), the dimension reduction method, and the tested classification methods, is described in Sect. 4. The experimental results and the comparison of the tested classifiers and different setups are discussed in Sect. 5, while Sect. 6 summarizes the results of the paper.

2 Related work

In the research of using inertial and magnetic sensors in human movement recognition systems, various types and positions of the sensors, and methods for recognition were tested for different applications (Ghasemzadeh et al. 2013). Classification is typically done in a two-stage process. First, features are derived from windows of sensor data. A

classifier is then used to identify the motion corresponding to each separate window of data.

Table 1 summarizes the applied activity classes, sensor types and their placements, feature extraction modes, processing window widths, sampling frequencies, classification methods, and achieved accuracies in relevant works. The used abbreviations are described in the following subsections.

2.1 Classes

In the related work, many activity classification approaches were used. The most widely used activities were standing and walking, which can be found in almost all works. Besides standing, other stationary activities can also be found in the literature, such as lying (Lee et al. 2011), sitting (Yang et al. 2009; Martin et al. 2013; Ugolotti et al. 2013),

Table 1 Summary of relevant works

Related work	Activity classes	Sensors and placement	Feature extraction	Processing window width /sampling frequency	Classifiers	Accuracy
Preece et al. (2009)	8 classes (moving, complex)	ACC: waist, thigh, ankle	TDFs FDFs Wavelets	2 s/64 Hz	k-NN	95%
Altun et al. (2010)	21 classes (stationary, moving, complex)	ACC, GYR, MAG: knees, wrists, chest	TDFs FDFs	5 s/25 Hz	PCA + BDM	99.1%
					PCA + SVM	98.6%
					PCA + DTW	98.5%
					PCA + k-NN	98.2%
					PCA + LSM	89.4%
					PCA + MLP	86.9%
					PCA + CT	81.0%
Lee et al. (2011)	6 classes (stationary, moving, complex)	ACC: chest	TDFs FDFs	10 s/20 Hz	LDA + MLP	94.43%
Zhu and Sheng (2011)	8 classes (stationary, transitional, moving)	ACC: right thigh	TDFs	1 s/20 Hz	MLP + HMM	80.88%
Fuentes et al. (2012)	4 classes (stationary, transitional)	ACC: chest	TDFs	1 s/100 Hz	SVM	94.73%
Varkey et al. (2012)	6 classes (stationary, moving, complex)	ACC, GYR: right wrist, right foot	TDFs	1.6 s/20 Hz	SVM	97.2%
Martin et al. (2013)	6 classes (stationary, moving, complex)	ACC, GYR, MAG: multiple places	TDFs FDFs	3 s/6.25 Hz (ACC), 100 Hz (GYR), 7.69 Hz (MAG)	CT	97%
					Decision table	88%
					NBC	78%
Chernbumroong et al. (2014)	13 classes (moving, complex)	ACC, GYR: dominant wrist	TDFs FDFs	3.88 s/33 Hz	SVM	97.2%
					MLP	96.73%
					RBF	95.67%
Li et al. (2014)	6 classes (stationary, moving, complex)	ACC: waist	TDFs	1 s/10 Hz	MLP	98.3%
					k-NN	94.1%
Attal et al. (2015)	12 classes (stationary, transitional, moving)	ACC: chest, right thigh, left ankle	TDFs FDFs Wavelets	1 s/25 Hz	k-NN	99.25%
					Random forest	98.95%
					SVM	95.55%
					SLGMM	85.05%
					HMM	83.89%
					GMM	75.60%
					k-means method	72.95%
Suarez et al. (2015)	6 classes (stationary, moving)	ACC, GYR: waist	TDFs	0.64 s, 1.28 s, 2.56 s/50 Hz	Lazy learner	99%
					CT	97%
					Rule-based classifier	97%
					NBC	84%
Korpela et al. (2016)	5 classes (moving, complex)	ACC: right wrist	TDFs FDFs	1 s/100 Hz	CT	97.8%

or both (Altun et al. 2010; Zhu and Sheng 2011; Attal et al. 2015; Suarez et al. 2015). Different transitional movements were also parts of the activity classes in some works, e.g. sit-to-stand and stand-to-sit (Zhu and Sheng 2011; Ugolotti et al. 2013; Attal et al. 2015), lie-to-sit and sit-to-lie (Zhu and Sheng 2011), lie-to-stand and stand-to-lie (Ugolotti et al. 2013), or stopping after walking (Fuentes et al. 2012). Regarding the classification of longer motional activities, various speeds and types of forward movements were also tested, such as slow, normal and rush walking (Martin et al. 2013), jogging (Preece et al. 2009; Yang et al. 2009; Varkey et al. 2012; Field et al. 2015), and running (Preece et al. 2009; Altun et al. 2010; Martin et al. 2013; Li et al. 2014; Korpela et al. 2016). Some works tried to differentiate different directions of an activity type, like level walking, walking downstairs and upstairs (Preece et al. 2009; Yang et al. 2009; Altun et al. 2010; Lee et al. 2011; Attal et al. 2015; Suarez et al. 2015) or walking backwards (Field et al. 2015). Yang et al. 2009 recorded even continuous rotational movements, such as walking left-circle or right-circle, and turning left or right. Special complex activities were also parts of the constructed databases, e.g. falling (Ugolotti et al. 2013; Li et al. 2014), jumping (Preece et al. 2009; Yang et al. 2009; Altun et al. 2010), writing (Varkey et al. 2012), brushing teeth (Bao and Intille 2004; Korpela et al. 2016), eating and drinking (Bao and Intille 2004), sweeping the floor, lifting a box onto a table, bouncing a ball (Field et al. 2015), driving (Lee et al. 2011), cycling (Bao and Intille 2004; Altun et al. 2010), etc.

2.2 Sensors and placement

The accelerometer (ACC) is the most popular sensor for monitoring the motion of the human body. This sensor measures acceleration in one or more axes. As seen in Table 1, many researchers used only a single unit to achieve activity recognition, but they differed in the placement of the sensor. Others applied multiple sensors fixed to different parts of the body. Beside the works listed in Table 1, Ugolotti et al. 2013 applied a single accelerometer fixed to the chest, Gonzalez et al. 2015 applied two accelerometer-based data loggers, which were mounted on each wrist, while Bao and Intille 2004 applied five biaxial sensors placed on each subject's right hip, dominant wrist, non-dominant upper arm, dominant ankle, and non-dominant thigh.

Gyroscopes (GYR), which measure angular velocity around one or more axes, are less popular in movement recognition applications, and are mostly used together with accelerometers. None of the related researches used only gyroscopes. Tri-axial accelerometers and gyroscopes used together provide six degrees of freedom (6DoF) sensor units. Yang et al. 2009 used measurement units containing a triaxial accelerometer and a biaxial gyroscope, and placed them to eight places on the body: the wrists, the ankles, the knees, the hip, and the left elbow.

The fusion of inertial sensors and magnetometers (MAG) is also reported in the literature. The magnetic sensors measure the Earth`s magnetic field, and thus, they are able to detect rotational movements compared to the magnetic north. Magnetic sensors are usually used together with the inertial sensors, which provides 9DoF measurement systems, but Maekawa et al. 2013 utilized only magnetometers for activity classification. The authors used sensor gloves with 9 magnetic sensors on both hands, and tried to classify simple (walking, running) and complex (shave, brush teeth, use electric toothbrush, etc.) activities. Lee and Cho 2016 applied the sensors of mobile phones for activity recognition, while Field et al. 2015 utilized an inertial motion caption system, comprised of 17 inertial sensors attached to different parts of the body. The 9DoF sensors were combined to get a global orientation through a Kalman Filter.

2.3 Feature extraction

As activity and movement recognition is a typical pattern recognition problem, feature extraction plays a crucial role during the recognition process. Sensor-based features can be classified into three categories: TDFs, frequency-domain features (FDFs), and features computed using time–frequency analysis.

Most of the related researches used TDFs and/or FDFs. The type of features and their frequency of usage in references are shown in Table 2. It can be concluded that the most used TDFs are the mean and the standard deviation, and the most frequent FDFs are the spectral energy and the frequency-domain entropy.

Using wavelet analysis, the signal is decomposed into a series of coefficients, which carry both spectral and temporal information about the original signal. Two works (Preece et al. 2009; Attal et al. 2015) tested this feature extraction method for the classification of activities. Preece et al. 2009 utilized the next features: the sum of the squared detail coefficients at different levels, the sum of the squares of the detail and wavelet packet approximation coefficients across different levels, the standard deviations and root mean square (RMS) values of detail and wavelet packet approximation coefficients at a few different levels, and the sum of the absolute values of coefficients at different levels. Attal et al. 2015 applied the following features: the sum of detail coefficients of wavelets, the sum of squared detail coefficients of wavelets, the energy of detail wavelets coefficients, and the energy of approximation wavelets coefficients.

Table 2 Used feature types in related works

Feature type	References
Time-domain features	
Standard deviation or variance	Preece et al. (2009), Altun et al. (2010), Lee et al. (2011), Zhu and Sheng (2011), Cohn et al. (2012), Fuentes et al. (2012), Guo et al. (2012), Varkey et al. (2012), Martin et al. (2013), Chernbumroong et al. (2014), Li et al. (2014), Attal et al. (2015), Suarez et al. (2015), Korpela et al. (2016)
Mean	Bao and Intille (2004), Preece et al. (2009), Altun et al. (2010), Lee et al. (2011), Zhu and Sheng (2011), Guo et al. (2012), Varkey et al. (2012), Martin et al. (2013), Chernbumroong et al. (2014), Li et al. (2014), Attal et al. (2015), Suarez et al. (2015), Korpela et al. (2016)
Root mean square	Varkey et al. (2012), Chernbumroong et al. (2014), Li et al. (2014), Attal et al. (2015), Korpela et al. (2016)
Correlation	Bao and Intille (2004), Lee et al. (2011), Varkey et al. (2012), Martin et al. (2013), Li et al. (2014)
Number of zero crossings	Cohn et al. (2012), Martin et al. (2013), Attal et al. (2015), Korpela et al. (2016)
Kurtosis	Altun et al. (2010), Guo et al. (2012), Chernbumroong et al. (2014), Attal et al. (2015)
Range	Fuentes et al. (2012), Varkey et al. (2012), Li et al. (2014), Attal et al. (2015)
Skewness	Altun et al. (2010), Guo et al. (2012), Chernbumroong et al. (2014), Attal et al. (2015)
Maximum	Varkey et al. (2012), Chernbumroong et al. (2014), Suarez et al. (2015)
Minimum	Chernbumroong et al. (2014), Suarez et al. (2015)
Number of rapid changes	Cohn et al. (2012)
Magnitude of the first peak of the autocorrelation	Cohn et al. (2012)
Frequency-domain features	
Frequency-domain entropy	Bao and Intille (2004), Preece et al. (2009), Lee et al. (2011), Martin et al. (2013), Chernbumroong et al. (2014), Attal et al. (2015)
Spectral energy	Preece et al. (2009), Maekawa et al. (2013), Martin et al. (2013), Li et al. (2014), Attal et al. (2015), Korpela et al. (2016)
Magnitude of the defined first few highest peaks	Preece et al. (2009), Guo et al. (2012), Maekawa et al. (2013), Chernbumroong et al. (2014)
Frequency of the defined first few peaks with highest amplitude	Altun et al. (2010), Guo et al. (2012), Maekawa et al. (2013)
Correlation between axes	Preece et al. (2009), Chernbumroong et al. (2014)
Median frequency	Cohn et al. (2012), Martin et al. (2013)
DC component	Attal et al. (2015)
Median power	Cohn et al. (2012)
Principal frequency	Preece et al. (2009)

2.4 Processing window width and sampling frequency

Windowing plays also a very important role during the extraction of features. Usually features are computed in fixed-size windows, which are shifted also with a fixed time. In the related work, the width of the applied processing windows is between 1 and 10 s, and the smallest size, 0.64 s, was tested by Suarez et al. 2015. The sampling frequency is also a very important factor in the processing phase. In relevant works, the applied frequencies were between 10 and 100 Hz.

2.5 Classifiers

The classification of the defined activities using the computed feature vectors can be done using different classification methods. As shown in Table 1, the most popular classifiers in relevant works are: support vector machines (SVM), the k-nearest neighbor (k-NN) method, decision trees or classification trees (CT), the naïve Bayes classifier (NBC), and multi-layer perceptron (MLP) neural networks. Some other methods were also tested, as radial basis function (RBF) neural networks, the least-squares method (LSM), Bayesian decision making (BDM), dynamic time warping (DTW), decision table, rule-based classifier, Gaussian mixture modeling (GMM), supervised learning GMMs (SLGMM), the k-means method, random forest, lazy learner, and hidden Markov models (HMMs). In some researches, the classifiers were used together with some dimension reduction methods. The most common methods are the principal component analysis (PCA) and the LDA. Guo et al. (2012) applied the generalized discriminant analysis (GDA) method with the multiclass relevance vector machine classifier. Some researchers even tested two different classification methods together: neural networks and HMMs (Zhu and Sheng 2011),

hierarchical temporal memories and SVMs (Ugolotti et al. 2013), CTs and HMMs (Maekawa et al. 2013), k-means clustering and HMMs (Lee and Cho 2016).

3 Experimental setup

The sensor devices used in body sensor networks must be designed with the aim of providing the highest degree of mobility for the patients. They must be small, lightweight, and wireless wearable units.

The used prototype system, which can be seen in Fig. 1 consists of an IRIS WSN mote, and a 9DoF digital sensor board connected to it. The IRIS mote is equipped with an Atmel ATmega 1281L 8-bit microcontroller, and an RF231 IEEE 802.15.4 compatible radio transceiver. The current draw of the microcontroller is 8 mA in active mode, and 8 µA in sleep mode, while the radio transceiver consumes 17 mA during transmission, and 16 mA during reception. The maximal data throughput of the radio transceiver is 250 kbps, and its outdoor range is over 300 m. The connected 9DoF sensor board is made up of an ADXL345 tri-axial MicroElectroMechanical System (MEMS) accelerometer, an ITG3200 tri-axial MEMS gyroscope, and an HMC5883L tri-axial magnetoresistive technology-based magnetometer. The ADXL345 is a low power accelerometer (the current draw is 40 µA in measurement mode, and 0.1 µA in sleep mode), which can measure up to ± 16 g in 13-bit resolution with the highest sampling rate of 3.2 kHz. The gyroscope features a 16-bit analog-to-digital converter, and it can measure angular rate in a range of ± 2000 deg/s with 8 kHz frequency. The normal operating current of the gyroscope is 6.5 mA, while the sleep mode current is 5 µA. The measurement range of the magnetic sensor is ± 8.1 Ga in 12-bit resolution with 160 Hz maximal sampling rate, and it consumes 2 µA current draw in idle mode, while 100 µA in measurement mode.

A TinyOS-based driver was developed and implemented to configure the sensors and cyclically read the measurement data. The data are read from the sensors via the I^2C interface, and sent via wireless communication to a BaseStation mote, which uses serial communication to forward the data to a PC.

3.1 Data acquisition

Eleven activities were defined in order to recognize specific arm movements in stationary positions and also during the movement of the body. The used activities are the following:

1. "standing without movement of the arms",
2. "sitting with the arms resting on a table",
3. "walking",
4. "turning around in one place",
5. "jogging",
6. "raising and lowering the left arm during standing",
7. "raising and lowering the right arm during standing",
8. "raising and lowering both arms during standing",
9. "raising and lowering the left arm during walking",
10. "raising and lowering the right arm during walking",
11. "raising and lowering both arms during walking".

Data were collected with the help of nine male subjects (ages between 20 and 50, and height between 165 and 190 cm) for all activities. The IRIS motes with the attached 9DoF sensor motes were mounted on each wrist of the subjects. The data were recorded in fixed-length sessions of 20 s for all activities using 125 Hz sampling frequency, which means 2500 measurements per sensor. The measurements were performed in a laboratory environment.

4 Classification algorithm

The classification is performed in four main stages. The software architecture with the four stages can be seen in Fig. 2. In the first step, the measurement data are preprocessed (Stage I.). In the second stage (Stage II.) features are extracted from the signals on each unit. Possible aggregation of the extracted features is also done in this stage.

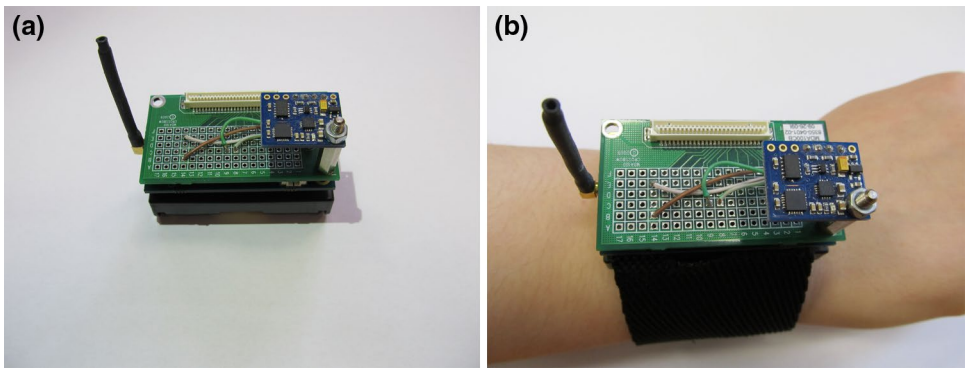

Fig. 1 **a** The prototype measurement system, **b** The unit attached to the wrist

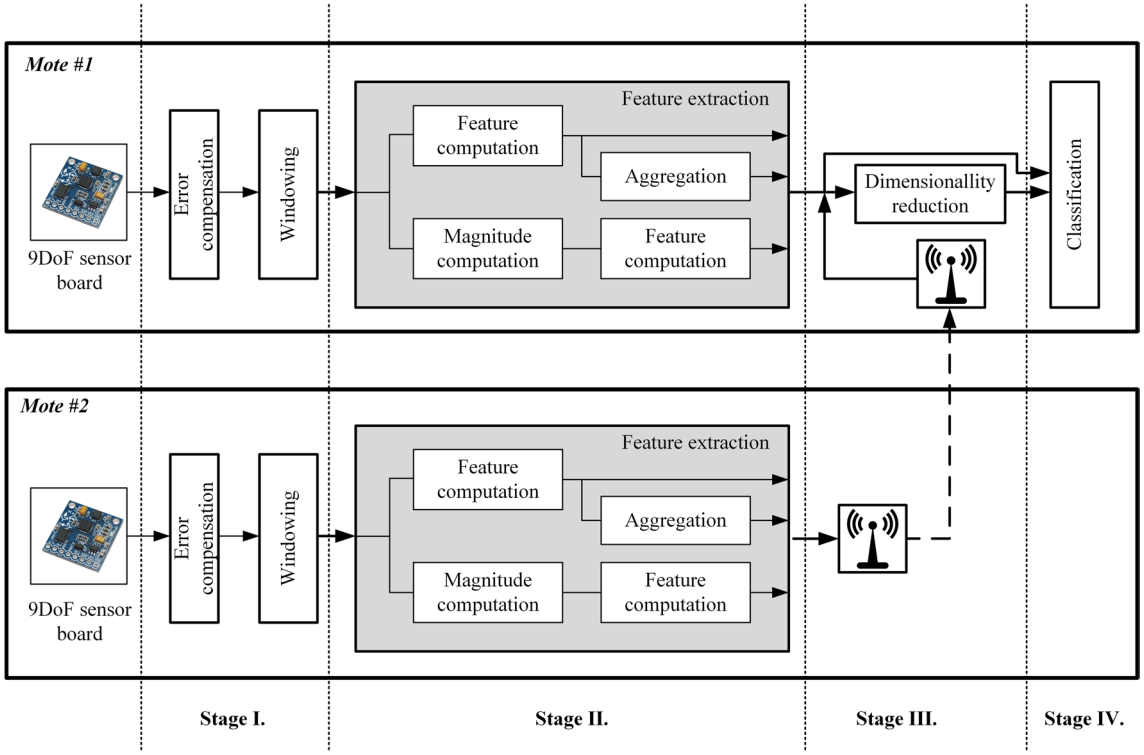

Fig. 2 Software architecture

The proposed algorithm assumes the transmission of the vector of the extracted features from one mote to the other, and the rest of the algorithm should be implemented in the microcontroller of the receiving device. Dimension reduction is done in the third stage (Stage III.), while classification is performed in the fourth stage (Stage IV.). Two different algorithms were applied and tested. In the first type, the third stage is not performed, and the classifiers receive the feature vectors directly, while in the second case the data sets are dimensionally reduced, so the classifiers have less input parameters. The advantage of the dimension reduction method is that it removes the redundant information.

4.1 Preprocessing

4.1.1 Error compensation

Due to high error rates caused by structural errors of the sensors, the raw measurements were compensated in the preprocessing phase. The calibration parameters (scale factors, offsets, and non-orthogonality errors) were obtained using an offline evolutionary algorithm-based method (Sarcevic et al. 2014). For the computation of the parameters, the algorithm uses measurements recorded in multiple stationary orientations.

4.1.2 Windowing

The extraction of feature values is performed in fixed-size segments, which are shifted with constant sizes. To generate a high number of input vectors, small window shifts were used. For hardware implementation, the size of the shifts depends on the available resources and the required response time, since the algorithm updates the movement classes after each window shift, and the reduction of the size of the shifts increases the necessary computation performance.

Both the CPU computation performance and the power resources are limited in IRIS WSN motes, so it is important to minimize the usage of these resources while maximizing the recognition efficiency. The required computation performance and the current draw of the sensors can be reduced if the sampling frequency is decreased.

4.2 Feature extraction

4.2.1 Feature types

The used features were chosen by their memory usage, required computation, and possible quantity of information. Due to easy implementation and low memory usage, only time-domain analysis was performed on the signals. Many of the chosen features were previously used for EMG pattern recognition (Phinyomark et al. 2012), and to

the best knowledge of the authors, most of them were not applied previously for movement classification. The used TDFs require only one or two previous measurements, so there is no need to store all the measurement data in the window as it is required for frequency domain analysis. But even standard deviation, which is the most frequently used features, requires the storage of the measurement vector in the window, since first the average needs to be calculated. The following TDFs were chosen for this research:

- *Mean Absolute Value (MAV)*: The calculation of the MAV feature can be expressed as follows,

$$\mathrm{MAV} = \frac{1}{N}\sum_{i=1}^{N}|x_i| \tag{1}$$

  where N is the number samples in the window, and x_i are the signal amplitudes at the given index.
- *Willison Amplitude (WAMP)*: The number of amplitude changes of incoming signals within a window, which are higher than a given threshold level. The computation of the WAMP can be expressed as

$$\mathrm{WAMP} = \sum_{i=1}^{N-1}[f(x_i - x_{i+1})], f(x)\begin{cases} 1, & \text{if}(x \geqslant \text{th}) \\ 0, & \text{otherwise} \end{cases} \tag{2}$$

  where *th* is the threshold, which is the peak-to-peak noise level.
- *Number of Zero Crossings (NZC)*: The number of times when the amplitude values cross the zero-amplitude level, and the difference between the values with opposite signs is larger than a defined threshold. The computation of the NZC feature can be represented as

$$\mathrm{NZC} = \sum_{i=1}^{N-1}\left[sgn\left(x_i \cdot x_{i+1}\right) \cap \left|x_i - x_{i+1}\right| \geqslant \text{th}\right],\ sgn(x) = \begin{cases} 1, & if(x \geqslant 0) \\ 0, & otherwise \end{cases} \tag{3}$$

- *Number of slope sign changes (NSSC)*: The number of direction changes, where among the three consecutive values the first or the last changes are larger than the predefined limit. The computation of this feature can be represented as follows,

$$\mathrm{NSSC} = \sum_{i=2}^{N-1}\left[f\left[\left(x_i - x_{i-1}\right)\cdot\left(x_i - x_{i+1}\right)\right]\right],\ f(x) = \begin{cases} 1, & if(x \geqslant th) \\ 0, & otherwise \end{cases} \tag{4}$$

- *Maximal (MAX) and minimal (MIN) value*: The highest and lowest measured value in the processing window.
- *RMS*: the calculation of the RMS in a processing segment can be done as.

$$\mathrm{RMS} = \sqrt{\frac{1}{N}\sum_{i=1}^{N}x_i^2} \tag{5}$$

- *Waveform length (WL)*: The cumulative length of the waveform over the time segment, which is calculated by the sum of absolute changes between two measurements:

$$\mathrm{WL} = \sum_{i=1}^{N-1}\left|x_{i+1} - x_i\right| \tag{6}$$

4.2.2 Extraction modes

The used input vectors were generated and tested with the use of two TDF calculation modes:

- *Separately used axes (SEP)*: the features are extracted separately for the X, Y, and Z axes of the sensors.
- *Vector magnitude-based (VL)*: the changes in the vector length are used for the computation of the TDFs. The advantages of this feature extraction mode are that three times less features are generated than with the SEP mode, and that it should be less sensitive to slight differences between movements of different subjects, or small displacements of the sensor motes on the wrists. However, it should not be able to recognize different poses in stationary positions. The magnitude-based feature extraction cannot provide valuable information in case of the magnetometer measurements, because the magnitude of the magnetic field is constant in ideal situations, thus, any measured distortions are caused by the changes in the indoor environment. Using the other two sensor types, the accelerometer and the gyroscope, this feature extraction mode can provide important information for the classification process. Except the NZC feature, which cannot give helpful information, since the magnitude cannot be negative, all other of the previously described TDF types can be effective.

4.2.3 Feature aggregation

The usage of the separately extracted features for the three sensor axes can result in a very high number of features, which can increase the complexity of the classification algorithm. Also, it can have a negative effect on the

recognition efficiency if the subjects do not fix the units correctly to their wrists. A possible solution to both previous problems can be the aggregation (AGG) of the separately computed features. As expressed in Eq. 7, this can be done by calculating a linear combination of the feature values computed for each axis for a specific feature type.

$$feat_{AGG} = w_X \cdot feat_X + w_Y \cdot feat_Y + w_Z \cdot feat_Z \tag{7}$$

where $feat_{AGG}$ is the aggregated feature value, $feat_X$, $feat_Y$, and $feat_Z$ are the extracted features for each axis, and w_X, w_Y, and w_Z are the corresponding weights.

4.3 Dimension reduction

The LDA method was used to perform dimensionality reduction on the datasets, which is a widely-used subspace learning method in statistics, pattern recognition and machine learning. This method aims to seek a set of optimal vectors, denoted by $W = [w_1, w_2, \ldots, w_m] \in \Re^{dxm}$, projecting the d-dimensional input data into an m-dimensional subspace, such that the Fisher criterion is maximized (Martinez and Kak 2001; Gu et al. 2011). The Fisher criterion, given in Eq. 8, aims at finding a feature representation, by which the within-class distance is minimized and the between-class distance is maximized.

$$\arg\max_{\boldsymbol{W}} \mathrm{tr}\Big(\big(\boldsymbol{W}^T \boldsymbol{S}_w \boldsymbol{W}\big)^{-1} \big(\boldsymbol{W}^T \boldsymbol{S}_b \boldsymbol{W}\big) \Big), \tag{8}$$

where $\boldsymbol{S}_b$ and $\boldsymbol{S}_w$ are the between-class scatter matrix and the within-class scatter matrix respectively, and are defined as

$$S_w = \sum_{j=1}^{c} \sum_{i=1}^{N_j} (x_i^j - \mu_j)(x_i^j - \mu_j)^T, \tag{9}$$

$$S_b = \sum_{j=1}^{c} (\mu_j - \mu)(\mu_j - \mu)^T, \tag{10}$$

where x_i^j represents the i-th sample of class j, $\boldsymbol{\mu}_j$ is the mean vector of class j, c is the number of classes, N_j is the number of samples in class j, and $\boldsymbol{\mu}$ is the overall mean vector of all classes. The mean vector of a class and the overall mean vector can be calculated as follows,

$$\boldsymbol{\mu}_j = \frac{1}{N_j} \sum_{i=1}^{N_j} \boldsymbol{x}_i^j, \tag{11}$$

$$\boldsymbol{\mu} = \frac{1}{c} \sum_{j=1}^{c} \sum_{i=1}^{N_j} \boldsymbol{x}_i^j. \tag{12}$$

The solution to the problem of maximizing the Fisher criterion is obtained by an eigenvalue decomposition of $S_w^{-1} S_b$, and taking the eigenvectors corresponding to the highest eigenvalues. There are *c-1* generalized eigenvectors. If the number of features is less than *c-1*, then the number of eigenvectors will be equal to the number of features.

4.4 Classification methods

In this research seven possibly applicable classification methods were chosen and tested:

- *Nearest Centroid Classifier (NCC)*: The NCC is used in various areas of pattern recognition because it is simple and fast. The method determines the Euclidean distance from an unknown object to the centroid of each class, and assigns the object to the class with the shortest distance. The Euclidean distance between the $x_i \in \Re^n$ feature vector and the n-dimensional $\boldsymbol{m}_j$ vector of mean values for class j can be calculated as

$$dist(\boldsymbol{x}, \boldsymbol{m}_j) = \sqrt{\sum_{i=1}^{n} \big(x_i - m_{ji}\big)^2} \tag{13}$$

- *MLP*: Artificial Neural Networks (ANNs) are inspired by the animal`s brain, and are used to approximate target functions (Mitchell 1997). The MLP is a feedforward ANN, where neurons are organized into three or more layers (an input and an output layer with one or more hidden layers), with each layer fully connected to the next one using weighted connections. A neuron has an activation function that maps the sum of its weighted inputs to the output. The o_j output of one node can be defined as

$$o_j = f\big(\boldsymbol{v}_j \cdot \boldsymbol{x} + b\big), \tag{14}$$

  where $\boldsymbol{x}$ is the input vector, $\boldsymbol{v}_j$ is the vector containing the weights, b is the bias value, and f is the applied activation function.

  Most commonly MLP networks are trained using the backpropagation algorithm, which employs gradient descent to attempt to minimize the squared error between target values and the network output values.
- *NBC*: The NBC is a highly practical Bayesian learning method. It is based on the simplifying assumption that, given the target value of the instance, the attribute values are conditionally independent, and the probability of observing the conjunction for attributes is just the product of the probabilities for the individual attributes (Mitchell 1997). Equation 15 presents the approach used by the NBC.

$$v_{NB} = \arg\max_{v_j \in V} P\big(v_j\big) \prod_i P\big(a_i | v_j\big) \tag{15}$$

where v_j denotes the target value output of the classifier, V is the finite set of target values, a_i are the attribute values, and $P(v_j)$ are the probabilities of v_j target values.

- *SVM*: In SVMs, a data point is viewed as a p-dimensional vector, and the goal is to separate such points with $(p\text{-}1)$-dimensional hyperplanes (Varkey et al. 2012). The hyperplane can be defined as

$$F(\boldsymbol{x}) = \boldsymbol{w} \cdot \boldsymbol{x} + b, \tag{16}$$

where x is the vector to be recognized, w is the normal vector to the hyperplane, and b determines the offset from the origin along the normal vector. Equation 17 defines the normal vector, and is subject to the condition expressed in Eq. 18.

$$\boldsymbol{w}^* = \sum_{i=1}^{l} \alpha^{i*} \cdot y^i \boldsymbol{x}^i, \tag{17}$$

where α^i is the i-th Lagrange multiplier, $y^i \in \{-1,1\}$, and l is the number of support vectors.

$$\alpha^{i*}\left[y^i\left(\boldsymbol{w}^{*T}\boldsymbol{x}^i + b^*\right) - 1\right] = 0, \ \forall \alpha^i \neq 0 \tag{18}$$

The function of the hyperplane is not suitable for solving linearly non-separable problems, or dealing with more than two classes. To classify data into multiple classes, two common methods can be used: "one-versus-one" (OvO) and "one-versus-all" (OvA).

- *k-NN*: The k-NN algorithm classifies the objects based on the closest training examples in the feature space (Altun et al. 2010; Li et al. 2014). To classify a new observation, the method finds the k nearest samples in the training data, and assigns the new sample to the class which provides the most neighbors. The Euclidean distance measure is used.
- *CT*: The CT is a rule-based algorithm, which uses a tree-like set of nodes for classifying inputs (Altun et al. 2010; Martin et al. 2013). The tree has predefined conditions at each node of the tree, and makes binary decisions based on these rules. The condition of the following node is checked until a leaf is found that contains the classification result.

5 Performance evaluation

Altogether 340 datasets were constructed using different combinations of used sensor types, TDF calculation modes, processing window sizes, and sampling frequencies.

The cost of the system can be decreased by decreasing the number of used sensor types, but in recognition efficiency their fusion can result in a drastic improvement. In order to explore the effect of the used sensor types in the application, seven sensor combinations were defined, since the three sensor types can be used alone, in pairs, and together. The SEP and AGG feature extraction modes were tested for all seven sensor combinations, while the VL mode was used only for the accelerometer and the gyroscope alone, and their data used together, since, as described in Sect. 4.2, the magnetometer data cannot provide valuable information using this feature extraction mode. Thus, 17 combinations were constructed using the applied sensor types and feature extraction modes.

The use of large processing windows can increase the required computation, and it can make harder the detection of transitions between activities. Since one of the goals of this research is to explore the recognition efficiency using processing windows in millisecond range, the following window width and shift pairs were tested: 80 ms width and 40 ms shift; 200 ms width and 40 ms shift; 400 ms width and 80 ms shift; 800 ms width and 80 ms shift.

The necessary computation can be lowered by decreasing the sampling frequency, but it can have a negative effect if any important spectral components disappear. The spectral analysis of the obtained measurements shows, that in case of the accelerometer and the gyroscope, the highest frequencies of the dominant spectral components are below 15 Hz, while in the case of the magnetometer data, no higher components can be noticed above 5 Hz. To find the optimal setup, where the chosen TDFs can be still effective, datasets were generated using five sampling frequencies: 25, 50, 75, 100, and 125 Hz. The data for the four lower frequencies were obtained by downsampling the measurement data collected with 125 Hz sampling frequency.

Data from five of the nine subjects were used for the training of the classifiers, while the data from the remaining four subjects were tested as unknown inputs for the validation of the trained classifiers. All six classification techniques were tested for all datasets with and without dimension reduction. No results could be achieved using the NBC without LDA, since some classes have features with zero variance.

In this study both the OvA and the OvO methods were tested and used for comparison in case of the SVM classifier.

The k-NN classification algorithm was tested with 1 to 10 neighbors. Analyzing the efficiencies on validation data, without dimension reduction a convergence (97%) can be noticed at 1–2 neighbors in almost 55% of the setups, while other setups mostly converge at 3–4 neighbors. With LDA 1–4 neighbors are needed to achieve convergence as well, but in most cases 4 neighbors are necessary.

The training of the MLP was tested using 1 to 15 neurons in the hidden layer. The 70% of the training data were used as training inputs, and 30% as validation inputs for the training method. The validation datasets were used as unknown inputs for testing the efficiency of the classifier. Hyperbolic

tangent sigmoid transfer function was used in the hidden layer, while the neurons in the output layer were created using the linear transfer function. The scaled conjugate gradient method was used for training. The results show that in both cases (with and without using LDA), at least 9 hidden layer neurons are needed to achieve convergence (97%), and in more than 70% of the setups 9–12 neurons were required. It can be also noticed, that without dimension reduction the distribution of the converge points is equal, while with LDA more setups converge at 9–10 neurons.

In the further comparison, the authors used the setup with the highest recognition rate on unknown samples for both the k-NN and the MLP algorithms.

5.1 Efficiency comparison of the classification methods

Table 3 summarizes the average rankings of the thirteen classification methods on training and validation data, and on weighted overall efficiencies. Since it is important to classify both the known and the unknown data correctly, the weighted efficiency was calculated using the sum of the achieved recognition rates on known and unknown data, but the efficiency on validation data was used with a double weight. The average ranking was computed using the ranking order of the methods for each of the 340 setups. The average efficiencies are also presented in Table 3. Comparing the rankings on validation data, it can be stated, that the MLP and the LDA-MLP methods are the most powerful classifiers. The MLP was the best in almost 48% of the datasets, and its average ranking is 2.85, while the average ranking of the LDA-MLP is 3.13. The NCC method achieved the worst results with an average of 10.67, but the LDA-CT, CT and OvO SVM methods had also poor results with a ranking above 9. The results obtained only on training data show, that the CT and the LDA-CT provide the highest results, with an average recognition rate of 96.58% and 94.46% respectively. They are followed by the LDA-k-NN (89.46%) and the k-NN (86.09%) algorithms. These classification techniques are designed to best fit on training data, but are not too efficient on unknown data. The MLP, which proved to be the best method in case of validation data, provided 82.00% efficiency on known datasets, and was fifth in the rankings. Analyzing the overall recognition, it can be seen, that the LDA-k-NN is the best classifier with an average ranking of 2.89. This method is followed by the MLP (3.62) and the LDA-MLP (4.36).

Rates for the 340 datasets when the tested classification techniques performed better without LDA, and the average rate of differences are tabulated in Table 4. It can be observed, that the LDA-based dimension reduction has in overall a slight negative effect on the efficiency of the MLP. It decreases the efficiency in around 70% of the datasets, but the differences are not significant. Also, very small differences can be noticed for the CT, but the dimension reduction decreases the ability to recognize known data for almost all setups, while in around half of the datasets it increases the overall efficiency and the recognition rate on validation data. The LDA method has a very positive effect on the other classification techniques. The most significant improvement was achieved with the NCC method, for which the application of dimension reduction increased the recognition rates in average by 10%. The obtained efficiencies were also higher in around 87% of the setups for all three compared result types. For the other three algorithms, higher classification rates were

Table 3 Average ranking and efficiency of different classification methods on different data types

Method	Average ranking on training data	Average ranking on validation data	Average ranking on weighted overall efficiencies	Average efficiency and standard deviation on training data (%)	Average efficiency on and standard deviation validation data (%)
CT	1.03	9.01	5.84	96.58 ± 3.09	58.91 ± 8.53
OvA SVM	11.22	9.86	10.61	44.97 ± 29.77	38.65 ± 24.17
OvO SVM	8.79	8.37	8.45	70.36 ± 18.75	58.41 ± 14.19
NCC	11.76	10.67	11.49	63.90 ± 13.71	56.46 ± 13.42
k-NN	4.69	6.96	6.28	86.09 ± 7.81	63.76 ± 9.96
MLP	5.63	2.85	3.62	82.00 ± 10.58	70.45 ± 8.82
LDA-CT	2.09	9.39	6.16	94.46 ± 3.72	60.33 ± 10.62
LDA-OvA SVM	10.28	7.95	9.11	72.30 ± 15.42	62.47 ± 13.80
LDA-OvO SVM	7.44	4.24	5.73	78.13 ± 14.26	67.05 ± 12.49
LDA-NCC	10.15	6.87	8.37	72.15 ± 15.87	62.83 ± 13.93
LDA-k-NN	3.32	4.46	2.89	89.46 ± 8.08	67.03 ± 11.42
LDA-MLP	6.49	3.13	4.36	80.84 ± 10.74	69.33 ± 9.53
LDA-NBC	8.10	7.21	8.08	77.16 ± 13.66	64.03 ± 11.64

Table 4 Effect of LDA-based dimension reduction on the tested classification techniques

Method	Higher results on training data (%)	Higher efficiency on validation data (%)	Higher weighted overall efficiency (%)	Average rate and standard deviation on training data (%)	Average rate and standard deviation on validation data (%)
CT	99.41	50.88	57.94%	2.29 ± 1.52	−1.31% ± 10.54
OvA SVM	40.00	38.53	40.59%	−36.85 ± 42.1	−36.45 ± 40.76
OvO SVM	41.18	25.29	33.82%	−8.81 ± 23.3	−11.83 ± 18.98
NCC	13.24	13.82	12.35%	−10.44 ± 12.93	−9.44 ± 12.18
k-NN	27.65	30.29	22.65%	−3.59 ± 5.51	−4.29 ± 9.13
MLP	75.88	64.71	67.35%	1.54 ± 3.67	1.86 ± 4.61

achieved in around 60–70% of the datasets both on training and validation data. The highest effect can be noticed on the OvA SVM, since without dimension reduction almost 37% lower efficiencies were obtained for both known and unknown data.

5.2 Efficiency comparison of the tested sampling frequencies and processing window sizes

The further comparison of the results, achieved with different sampling frequencies and window sizes, was done using the best achieved overall weighted efficiencies.

The results show, that using the five tested sampling frequencies, the average difference between the highest and lowest efficiencies is 6.74 ± 8.47% for training data, and 6.83 ± 6.45% for validation data. The impact of increasing the sampling frequency is almost the same for the four different processing window sizes, but it has different effect on the 17 combinations of extraction modes and used sensors. Analyzing results on validation data, larger differences can be noticed when the magnetometer is used alone. In case of the SEP mode, the difference between the largest and smallest efficiency is 3–7%, and the recognition rate is decreasing with the increasing of the sampling frequency. The other setups provide almost constant efficiency or a rising tendency by increasing the sampling frequency. The AGG setup provides differences between 2.5% and 4.5% using only the magnetometer data, and around 3% for the data of the angular velocity sensor. Higher differences, can be also observed when the SEP feature extraction is performed on the fused data of the magnetic sensor and the gyroscope (3–5.7%), when the AGG features are applied on the data of the magnetometer and the accelerometer together (2.5–8%), and when the data of the accelerometer and gyroscope are used together and VL-based feature extraction is done (3.2-6%). The other setups provided below 2% differences.

The size of the processing window width has a more significant effect on recognition rates, since the larger windows always result in higher efficiency. In overall, the highest classification efficiencies are higher than the lowest rates for 13.24 ± 6.34% on training data, and 28.1% ±14.48% on validation data. The improvements do not differ greatly for different sampling frequencies, but they are more significant in case of the 17 different combinations of sensors and feature extraction modes. Especially high differences on validation data can be noticed for the three setups when the VL-based feature computation was used: gyroscope—27.6–29.2%, accelerometer—18.7–27%, and the gyroscope and the accelerometer together—26-28.6%. The lowest improvements can be observed in case of the two setups when the three sensors were used together: SEP—9.7–11.1%, AGG—7.1–9.5%. The increasing of the window size also has lower effect in case of the gyroscope when the features are computed using the SEP and AGG methods, 11.5–12.5% and 6.4–12.5% respectively, and when the SEP technique is used on the fused data of the gyroscope and the accelerometer, where the differences are between 10.4 and 12.8%.

5.3 Efficiency comparison of the tested feature extraction modes and sensor combinations

The best results for the 17 different combinations in the four different processing window widths can be seen in Fig. 3. It can be observed, that using only the magnetic sensor with the AGG feature extraction can provide the lowest recognition rates, since with the smallest window size only 39.95% can be achieved, while with even the largest processing window the efficiency increases only to 60.05%. Using the SEP mode, the recognition rates are much higher, 57.03% with the 80 ms window and 67.18% with the 800 ms window size.

Using only the angular rate sensor provides the highest results with the SEP method: 66.6–80.7%. The VL mode provides smaller classification rates, but the difference decreases by increasing the size of the processing window, since with the smallest window size the difference is 20%, while with the largest window a recognition rate of 78.33% can be achieved, which is only 2.37% lower than with the SEP mode. The number of features was 48 for the SEP mode and 14 for the VL mode, which is a significant difference. Using the AGG extraction mode, for which the

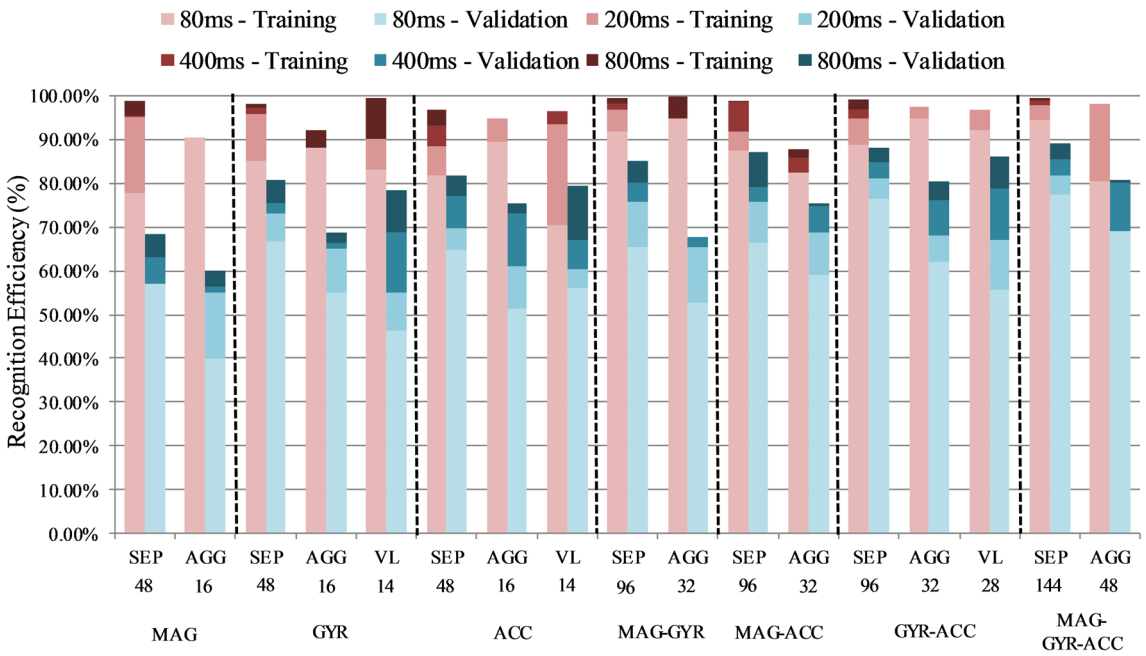

Fig. 3 Achieved classification efficiencies on training and validation data using different processing window sizes. The horizontal axes show the feature extraction mode in the first row, the required feature numbers in the second row, and the used sensor types in the third row (MAG-magnetometer, ACC-accelerometer, and GYR-gyroscope)

size of the feature vector was 16, significant difference to the VL mode can be noticed for the smaller window sizes. The recognition efficiency was 8,5% higher for the 80 ms window, and 10,18% for the 200 ms window, but for the two larger sizes the VL achieved better results, 2.55% and 9.57% respectively.

Using only the accelerometer, similar results can be achieved as with the gyroscope. For the two smaller windows with the SEP and AGG modes the accelerometer performed lower results, while with increasing the window size, the accelerometer provides higher efficiencies than the gyroscope. For the SEP mode, the differences were 1–3%, but for the two smaller windows with the AGG mode the recognition rates are lower for 3–5%, and higher for the two larger windows for 7%. With the VL-based feature vectors the accelerometer provides better results. Using the 80 ms processing window size the difference was around 10%, but the difference decreases, and was only 1% for the 800 ms window.

The usage of the magnetometer itself cannot provide usable results, but it can improve the performance of the inertial sensors, since the largest classification rates are 85.03% and 87.2% respectively. In case of the gyroscope, in average, the results were improved for 3.26% ±3.59% for the SEP mode, while with the accelerometer it provides an improvement of 5.11% ±3.19% for the SEP, and 7.45% ±7.44% for the AGG mode. For the setup where the data from the magnetometer and the gyroscope were fused, and the AGG feature extraction mode was performed, in average the results were even slightly lower than when the data from the gyroscope was used alone.

The highest recognition rate on validation data, 89.14% (99.48% on training data), was reached using all three sensor types with the SEP feature extraction in the largest processing window. This setup requires the usage of 144 features. With the same extraction mode, but without using the magnetic sensor, 87.96% classification efficiency can be achieved on validation data, and 98.91% on training data, with a required feature number of 96. By decreasing the size of the processing window, the classification rate significantly decreases, but even with the smallest window, an efficiency of 77.32% can be achieved with, and 76.5% without the magnetometer. The difference between these two setups is a little above 1% in efficiency, but the number of features, the energy consumption, and the cost are all increased if the magnetic sensor is added to the system. Similar differences can be noticed with the AGG extraction mode also.

The setup where the features were computed using the VL-based extraction, and the data from the angular velocity sensor and the accelerometer were used together, also proved to be very useful. The feature vectors consisted of 28 different features, and with the largest processing window the recognition rate was 86.17%. This extraction mode fails when the processing windows are small, since the efficiency with the 80 ms size was only 55.8%, and the AGG-based features provide higher efficiencies in these cases.

5.4 Training time comparison of the classification methods

Training time is not a crucial factor for the implementation of a classifier, but it can prove to be very important, especially when different combinations of features should be tested. To generate comparable data, all trainings were done on the same PC with the next characteristics: Intel core i7 3.5 GHz processor, 16 GB RAM, GeForce GTX 770 video card.

The computation of the LDA matrices proves to be very fast, and even for the largest setup, which contains 144 inputs, less than 1.8 s is required.

The k-NN method does not require any training, since it uses the entire dataset for the classification. The shortest, longest, and mean training times for the other classification methods are summarized in Table 5. It can be stated, that the most time consuming from the tested classification methods is the OvA SVM algorithm, since the training of the larger setups can last for more than 2 h, but even the shortest time was almost 1 min. The OvO SVM method proves to be much faster, but the longest time is still above 1 h, while the shortest is 17 s. The dimension reduction has a significant impact on the SVM-based methods, since it decreases the training time by 93.51% ±11.4% for the OvA, and by 92.45% ±10.79% for the OvO method. Beside the high reduction in training time, caused by the LDA, the longest required intervals are still too high for both methods. The training of the CT method requires between 0.37 and 15 s, and the LDA method does not reduce the training time for all setups, but the longest training was three times shorter than without the dimension reduction. The computation of the parameters for the NCC classifiers is very low for low dimension setups, but for the largest setups it can last for even 25 s. The effect of the LDA can be noticed only at the larger setups, and it reduces the maximal time to 2 s. The training of the LDA-NBC classification method, similarly to the LDA-NCC, lasts between a few hundredths and 2 s. The training of the MLP classifiers is also very time-consuming. The longest interval using 10 hidden layer neurons was 1331.6 s. Besides, that even the length of only one training is long, to find the optimal setup, multiple trainings are required with different neuron numbers in the hidden layer. This significantly increases the required training time. The LDA-based dimension reduction has a significant effect on this classification method, since it reduces the longest training time to 97.83 s, and in average it reduces the training time by 48.43 ± 34.92%.

Table 5 Smallest, highest, and mean required training times of the tested classification methods

Method	Shortest training time (s)	Longest training time (s)	Mean training time (s)
CT	0.37	15.01	3.41
OvA SVM	57.64	7415.20	3352.70
OvO SVM	16.99	3791.40	1414.70
NCC	~0	2.12	0.24
MLP	10.16	1331.60	84.81
LDA-CT	0.59	5.30	1.86
LDA-OvA SVM	8.28	2576.20	194.2
LDA-OvO SVM	2.43	860.70	52.38
LDA-NCC	0.03	24.90	1.64
LDA-MLP	6.36	97.83	26.71
LDA-NBC	0.06	2.18	0.34

5.5 Memory requirement comparison of the classification methods

The required space for the implementation of a classifier is a very important factor, since microcontroller-based systems have limited amounts of memory.

The required number of parameters for the implementation of the NBC, the NCC, and the MLP classifiers can be calculated using the number of features and classes. The number of hidden layer neurons is also needed in case of the MLP-based methods. In case of the k-NN, the number of samples in the classes is required, since the algorithm uses the entire feature set to determine the class. The required memory for the SVMs and the CTs cannot be calculated as a function of the number of features and classes, because the number of necessary support vectors in case of SVMs and necessary nodes in case of CTs differs. For comparison, the required memory spaces were calculated in bytes (1 floating-point number is equal with 4 bytes).

The LDA projection matrices have 10 rows, because 11 classes are used, and the number of columns is equal to the number of features. If the number of features is less than 10, the number of rows will be equal to the number of features.

The training of the NCC was performed by calculating the mean values of different features for each class, and the highest and smallest feature values were also needed for normalization when the dimension reduction was not used.

For the implementation of MLPs, input ranges, weights and biases are needed. The input ranges consist of the highest and lowest values for all inputs, and are used for normalization. Two weight matrices are needed to connect the input layer with the hidden layer, and the hidden layer with the output layer. The first consists of $num_{\mathrm{HiddenLayerNeurons}} \bullet num_{\mathrm{InputLayerNeurons}}$, while the second of $num_{\mathrm{OutputLayerNeurons}} \bullet num_{\mathrm{InputLayerNeurons}}$ weights. Bias values are used in all neurons of the hidden and the output layer. For comparison, based on the convergence in efficiency, 10 hidden layer neurons were used for the computation of the required memory.

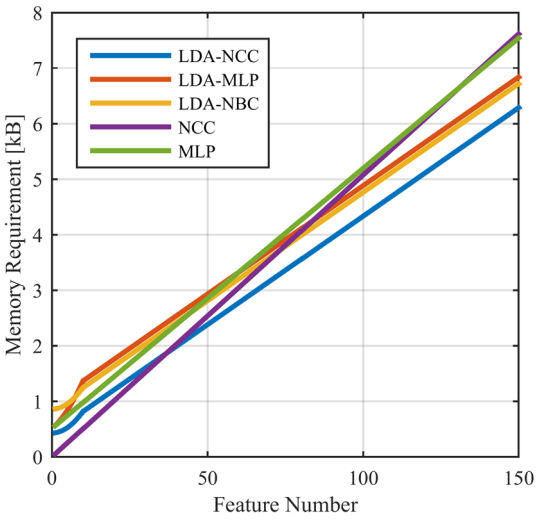

Fig. 4 Memory requirement of the classification methods with determinable memory consumption

Table 6 Highest and lowest memories required for implementation for the CT, OvA SVM, and the OvO SVM, with and without LDA-based dimension reduction

Method	Lowest required memory (kB)	Highest required memory (kB)
CT	2.03	83.45
LDA-CT	6.67	84.86
OvA SVM	652.36	27458.01
LDA-OvA SVM	213.85	2358.40
OvO SVM	369.30	17913.09
LDA-OvO SVM	106.16	1176.95

The training of the NBC results in a $num_{\text{Classes}} \bullet num_{\text{Features}}$ sized array of parameter pairs, where the first parameter is the mean deviation, and the second is the standard deviation.

The memory requirements of the five determinable methods can be seen in Fig. 4. It can be observed that they do not differ significantly. Considerable differences can be noticed only with a small number of features, e.g. with using 80 features, all methods require around 4 kbytes of parameters, but with only 10 features the LDA-MLP needs around 1.5 kbytes, while the NCC only 0.5 kbytes, which is three times lower. Generally, the LDA-NCC needs the least memory space, only the NCC needs less when the number of features is smaller than 40.

The k-NN method is a very memory demanding method, since the entire database of features is needed for its implementation. In this research, more than 13,000 feature vectors were used even in the smallest setups, which would result in more 760 kB memory space for a feature number of 15.

The highest and lowest required memories for the CT and SVM-based methods can be seen in Table 6.

The implementation of the CTs requires the number of nodes (16-bit integer), parents (one 16-bit integer per node), children (two 16-bit integers per node), cut points (one floating-point number per node), cut types (one Boolean value per node), and cut predictors (one 8-bit number per node). Analyzing the results, it can be stated, that the required number of nodes and the classification efficiency are inversely proportional. As showed in Table 6, the achieved smallest needed memory space is 2.03 kB, but high deviations can be noticed, and for the setup with most required nodes more than 83 kB of storage is needed. The LDA has a negative effect on the CT for all setups, and even the lowest required memory is 6.67kB. In average the LDA increases the required memory space by $60.44 \pm 42.64\%$.

In case of the SVM-based methods, due to the used 11 classes, the OvA method needs 11 support vector sets, while for the OvO $\text{num}_{\text{Classes}} \bullet (\text{num}_{\text{Classes}} - 1)/2$ sets are needed, what means 55 sets for the used 11 classes. The support vector sets are made up of different numbers of support vectors and a bias value. The dimension of each support vector is equal to the number of features, and they also include an alpha value. The obtained results show that both the OvA and OvO methods require a very high number of parameters for implementation, and thus, are not suitable for application in the developed system. The required memory space is less for the setups with higher efficiency rates, and it decreases by increasing the size of the processing window, since the classification rates increase. The lowest memory requirement, as shown in Table 6, was 652.36 kB for the OvA mode, and 369 kB for the OvO mode. In some setups, it can be even above 20 MB using the OvA mode. The LDA has a very positive effect on the SVM classification algorithm, since it greatly decreases the required number of support vectors. The tested dimension reduction method decreases the number parameters for all setups in case of the OvA SVM method, with an average of $55.91 \pm 27.03\%$, while for the OvO SVM it reduced the memory consumption for 65.29% of the setups.

5.6 Comparison with frequency-domain features

To explore the capabilities of the applied TDFs, it was reasonable to compare the achieved results with recognition rates obtained with FDFs used in the literature. The following FDFs were utilized in the feature sets: spectral entropy, spectral energy, magnitude of largest peak, frequency of largest peak, median frequency, DC component, median power, and principal frequency. Two TDFs, which require the storage of the measurement vectors for their computation, were also added to the datasets: standard deviation and correlation between axes. Feature extraction was performed

on the sensor axes separately and on the magnitude, and the aggregation-based feature reduction was also applied. Classification was done using the MLP classifier, which earlier proved to be the most powerful method.

The obtained results show, that the applied TDFs have better performance in around 60% of the datasets in case of the training data, while the rates are nearly equal on validation data. The rates, when the TDFs perform better on training data, are nearly equal for both different sampling frequencies and different processing window widths. In case of the validation data, the rates show a rising tendency when the sampling frequency or the size of the window is increased. With the smallest frequency or window size, TDFs give better results in around 40% of the datasets, while this rate is almost 60% with the largest frequencies or windows. Since the number of measurements in the processing window increases both with increasing the sampling frequency or the size of the processing window, this is a significant result, because the chosen TDFs do not require the storage of the measurement values in the window.

Table 7 Achieved classification efficiencies applying extraction based on TDFs and FDFs

Used sensors	Extraction mode	Feature type and number	Processing window width							
			Dataset							
			80 ms		200 ms		400 ms		800 ms	
			TR (%)	VA (%)	TR (%)	VA (%)	TR (%)	VA (%)	TR (%)	VA (%)
MAG	SEP	TD-48	74.54	52.43	85.76	59.95	91.27	63.23	96.36	69.97
		FD-60	80.86	44.76	84.89	50.45	88.35	57.41	95.98	58.31
	AGG	TD-16	67.38	48.50	73.14	55.40	74.15	55.25	77.37	58.50
		FD-20	61.65	46.45	68.20	53.88	71.50	56.93	76.04	59.62
GYR	SEP	TD-48	69.93	62.47	84.09	70.90	84.25	72.86	94.05	76.39
		FD-60	77.61	69.98	82.52	76.29	91.14	78.76	90.14	82.83
	AGG	TD-16	62.56	58.03	71.32	65.37	68.51	63.86	74.71	69.21
		FD-20	63.15	60.30	68.97	65.42	70.10	69.55	72.63	71.42
	VL	TD-14	56.82	52.60	62.19	58.89	74.81	68.35	84.61	79.39
		FD-18	56.54	52.34	65.60	61.65	73.94	68.56	80.82	74.77
ACC	SEP	TD-48	72.90	65.77	84.60	73.83	87.67	76.61	90.75	82.12
		FD-60	76.07	65.08	83.00	72.55	88.17	76.90	94.30	83.11
	AGG	TD-16	66.96	63.62	76.42	69.34	77.35	72.95	79.39	74.28
		FD-20	57.74	52.48	67.04	58.94	68.84	66.83	72.34	70.96
	VL	TD-14	53.47	53.51	64.08	62.78	77.60	73.50	82.46	79.47
		FD-18	54.22	52.89	62.74	60.82	71.80	72.23	79.12	80.31
MAG GYR	SEP	TD-96	89.80	67.53	94.06	70.71	96.70	72.92	83.85	74.25
		FD-120	92.08	64.55	93.92	70.78	95.98	74.81	99.57	79.06
	AGG	TD-32	79.68	61.44	83.05	64.51	84.76	67.53	85.34	70.99
		FD-40	80.01	68.63	83.79	72.38	84.97	74.95	84.94	77.95
MAG ACC	SEP	TD-96	84.35	68.32	86.41	74.34	96.20	77.25	98.43	83.98
		FD-120	88.11	58.10	92.41	64.63	95.67	69.38	98.87	73.36
	AGG	TD-32	75.77	67.86	83.17	71.45	85.05	73.78	86.28	74.79
		FD-40	72.68	56.81	77.01	66.84	80.64	66.48	83.88	70.73
GYR ACC	SEP	TD-96	88.13	76.60	88.80	80.57	95.50	83.25	98.33	84.69
		FD-120	86.13	77.94	89.27	81.64	91.01	84.63	98.63	87.38
	AGG	TD-32	74.77	68.64	80.80	74.99	81.24	76.29	81.67	78.00
		FD-40	69.72	66.61	77.59	74.20	80.38	75.79	80.76	76.94
	VL	TD-28	67.46	61.31	76.17	71.07	84.08	78.45	91.51	85.61
		FD-36	67.45	62.95	76.90	71.02	80.88	75.10	89.81	82.74
MAG GYR ACC	SEP	TD-144	93.98	74.23	93.98	79.11	97.16	81.91	98.70	84.22
		FD-180	93.34	68.63	95.73	74.75	98.30	80.71	98.98	82.51
	AGG	TD-48	80.94	69.59	87.01	76.04	88.14	75.95	90.33	78.53
		FD-60	82.32	70.27	84.63	74.83	86.63	75.85	87.42	77.65

Table 7 summarizes the obtained results with MLPs using TDFs and FDFs when the highest sampling frequency, 125 Hz, was applied. The used abbreviations are the next: TR – training data, VA – validation data, TD – time-domain, FD – frequency domain.

The recognition rates achieved with FDFs, just like with TDFs, increase with the increasing of the sampling frequency or the processing window width. The highest classification efficiency on validation data, 87.38%, was achieved using the gyroscope and the accelerometer data together, and applying the SEP extraction mode. It should be noted, that, as it can be seen in Table 7, the number of applied features is considerably higher in the datasets based on FDFs. The average difference between efficiencies obtained on validation data utilizing TDFs and FDFs is around 3%, while the highest differences, around 11%, can be noticed when features are extracted from the measurements of the magnetometers.

Analyzing the classification efficiencies using different feature extraction modes, it can be concluded, that the aggregation-based feature reduction is also useful when FDFs are applied. The features computed from the accelerometer measurements provide better recognition rates using TDFs, but both the gyroscope and the magnetometer give even better results with FDFs in case of the AGG-based extraction. The magnitude-based extraction results in similar recognition efficiencies using TDFs and FDFs.

6 Conclusion

In this study, a wearable prototype measurement system was presented, which uses 9DoF sensor boards mounted on WSN motes. A new classification algorithm was also proposed, which utilizes two wrist-mounted sensor motes to detect different arm movements in stationary positions, and during the movement of the body. The major advance of the proposed algorithm is that the processing can be easily implemented on the microcontroller of the wearable unit. The measurement system can be realized in a wristwatch-like unit for real life applications.

To explore the optimal cost, power consumption, and efficiency, 340 datasets were constructed based on different feature extraction modes, sampling frequencies, processing window sizes, and sensor combinations. To reduce computation costs, only time-domain features with low memory requirements were applied. The accelerometer, the gyroscope, and the magnetometer were tested separately, in pairs, and altogether, to investigate the impact of the sensors in the application, and to prevent unnecessary usage of memory and hardware resources, and of course, it can lower the overall cost and power consumption of the system.

The results show that the recognition rates achieved, using only simple time-domain features, are not affected significantly by the sampling rate, and only slight improvements can be noticed when it is increased. The tested millisecond range processing windows prove to be usable, since above 77% percent efficiency can be reached on unknown data even with the smallest, 80 ms, window width, while almost 90% can be achieved with the 800 ms window size. It can be concluded from the achieved efficiencies, that the movements of different subjects show high correlation, since the training and validation datasets were constructed of data from different persons. The classification rates on training data can be almost 100%, which is also a very important factor if the application should be trained and used for one person.

The magnetic sensor itself provides very low, 40–67%, recognition rates, but it can significantly improve the performance of the gyroscope and the accelerometer if they are used together. The two inertial sensors alone can provide around 80% applying the largest processing window. The highest efficiencies were achieved when the data from the three sensor types were applied together, but the impact of the magnetometer is very small, since it only increases the recognition rates by 1–2%, while it largely increases the cost, the energy consumption, and the required feature number.

The highest efficiencies were achieved when the separately computed features were used, but they require three-times more used features than the aggregation- and magnitude-based datasets. The inertial sensors can provide 86.17% using the VL-based extraction in the 800 ms processing window, but for the smaller window sizes the proposed aggregation-based feature extraction provides higher classification rates.

Seven popular classification methods, the MLP, the NCC, the NBC, the OvA SVM, the OvO SVM and the k-NN, were tested with and without LDA-based dimension reduction. The classifiers were compared by efficiency, training time, and memory requirement for implementation. The obtained results show that the LDA can lower memory consumption and/or training time, but it can also increase classification efficiency of some classifiers. It can be concluded that the highest efficiency can be achieved using the MLP classifier, but the use of the LDA-MLP is also reasonable due to the slightly lower efficiency, lower memory requirements in case of high feature numbers, and significantly lower training time. The CT can effectively classify the training data, but its performance is significantly lower for the unknown samples. The very popular k-NN and SVM-based methods showed to be unsuitable for use in this application due to their low efficiencies and high hardware requirements.

The tested TDFs were also compared to FDFs utilized in the literature. The results show, that the TDFs perform better when the number of measurements is increased in the processing window, which is a significant result, since the chosen TDFs do not require the storage of the measurement data. The proposed aggregation-based feature reduction is also useful in the case of the FDFs, since for some extraction modes, the obtained recognition rates are even higher than achieved using TDFs.

The future goals of this research include distributing the algorithm on the two motes, finding optimal weights for the aggregation based feature extraction, as well as finding the features with the most influence. The proposed system could also be easily expanded for the detection of falls and epileptic seizures.

Acknowledgements The publication is supported by the European Union and co-funded by the European Social Fund. Project title: "Telemedicine-focused research activities on the field of Mathematics, Informatics and Medical sciences" Project number: TÁMOP-4.2.2.A-11/1/KONV-2012-0073.

Compliance with ethical standards

Conflict of interest The authors declare that they have no conflict of interest.

References

Aiello F, Bellifemine FL, Fortino G, Galzarano S, Gravina R (2011) An agent-based signal processing in-node environment for real-time human activity monitoring based on wireless body sensor networks. Eng Appl Artif Intell 24:1147–1161. doi: 10.1016/j.engappai.2011.06.007

Alemdar H, Ersoy C (2010) Wireless sensor networks for healthcare: A survey. Comput Netw 54:2688–2710. doi: 10.1016/j.comnet.2010.05.003

Altun K, Barshan B, Tuncel O (2010) Comparative study on classifying human activities with miniature inertial and magnetic sensors. Pattern Recognit 43:3605–3620. doi: 10.1016/j.patcog.2010.04.019

Attal F, Dedabrishvili M, Mohammed S, Chamroukhi F, Oukhellou L, Amirat Y (2015) Physical human activity recognition using wearable sensors. Sens 15:31314–31338. doi: 10.3390/s151229858

Bao L, Intille S (2004) Activity recognition from user-annotated acceleration data. Lect Notes Comput Sci 3001:1–17. doi: 10.1007/978-3-540-24646-6_1

Chernbumroong S, Cang S, Yu H (2014) A practical multi-sensor activity recognition system for home-based care. Decis Support Syst 66:61–70. doi: 10.1016/j.dss.2014.06.005

Cohn G, Gupta S, Lee TJ, Morris D, Smith J, Reynolds M, Tan D, Patel S (2012) An ultra-low-power human body motion sensor using static electric field sensing. In: Proceedings of the ACM Conference on Ubiquitous Computing (UbiComp), pp 99–102

Cornacchia M, Ozcan K, Zheng Y, Velipasalar S (2017) A survey on activity detection and classification using wearable sensors. IEEE Sens J 17:386–403. doi: 10.1109/JSEN.2016.2628346

Field M, Stirling D, Pan Z, Ros M, Naghdy F (2015) Recognizing human motions through mixture modeling of inertial data. Pattern Recognit 48:2394–2406. doi: 10.1016/j.patcog.2015.03.004

Fuentes D, Gonzalez-Abril L, Angulo C, Ortega JA (2012) Online motion recognition using an accelerometer in a mobile device. Expert Syst Appl 39:2461–2465. doi: 10.1016/j.eswa.2011.08.098

Ghasemzadeh H, Ostadabbas S, Guenterberg E, Pantelopoulos A (2013) Wireless medical-embedded systems: A review of signal-processing techniques for classification. IEEE Sens J 13:423–437. doi: 10.1109/JSEN.2012.2222572

Gonzalez S, Sedano J, Villar J, Corchado E, Herrero A, Baruque B (2015) Features and models for human activity recognition. Neurocomputing 167:52–60. 10.1016/j.neucom.2015.01.082

Gravina R, Alinia P, Ghasemzadeh H, Fortino G (2017) Multi-sensor fusion in body sensor networks: State-of-the-art and research challenges. Inf Fusion 35:68–80. doi: 10.1016/j.inffus.2016.09.005

Gu Q, Li Z, Han J (2011) Linear discriminant dimensionality reduction. Lect Notes Comput Sci 6911:549–564. doi: 10.1007/978-3-642-23780-5_45

Guo Y, He W, Gao C (2012) Human activity recognition by fusing multiple sensor nodes in the wearable sensor systems. J Mech Med Biol. doi: 10.1142/S0219519412500844

Korpela J, Maekawa T, Eberle J, Chakraborty D, Aberer K (2016) Tree-structured classifier for acceleration-based activity and gesture recognition on smartwatches. In: IEEE International Conference on Pervasive Computing and Communications Workshops

Lee Y-S, Cho S-B (2016) Layered hidden Markov models to recognize activity with built-in sensors on Android smartphone. Pattern Anal Applic 19:1181–1193. doi: 10.1007/s10044-016-0549-8

Lee MW, Khan AM, Kim TS (2011) A single tri-axial accelerometer-based real-time personal life log system capable of human activity recognition and exercise information generation. Pers Ubiquitous Comput 15:887–898. doi: 10.1007/s00779-011-0403-3

Li C, Lin M, Yang L, Ding C (2014) Integrating the enriched feature with machine learning algorithms for human movement and fall detection. J Supercomput 67:854–865. doi: 10.1007/s11227-013-1056-y

Maekawa T, Kishino Y, Sakurai Y, Suyama T (2013) Activity recognition with hand-worn magnetic sensors. Pers Ubiquitous Comput 17:1085–1094. doi: 10.1007/s00779-012-0556-8

Martin H, Bernardos A, Iglesias J, Casar J (2013) Activity logging using lightweight classification techniques in mobile devices. Pers Ubiquitous Comput 17:675–695. doi: 10.1007/s00779-012-0515-4

Martinez A, Kak A (2001) PCA versus LDA. IEEE Trans Pattern Anal Mach Intell 23:228–233. doi: 10.1109/34.908974

Mitchell T (1997) Machine learning. McGraw-Hill, New York

Phinyomark A, Phukpattaranont P, Limsakul C (2012) Feature reduction and selection for EMG signal classification. Expert Syst Appl 39:7420–7431. doi: 10.1016/j.eswa.2012.01.102

Preece S, Goulermas JY, Kenney L, Howard D (2009) A comparison of feature extraction methods for the classification of dynamic activities from accelerometer data. IEEE Trans Biomed Eng 56:871–879. doi: 10.1109/TBME.2008.2006190

Sarcevic P, Pletl S, Kincses Z (2014) Evolutionary algorithm based 9DOF sensor board calibration. In: IEEE International Symposium on Intelligent Systems and Informatics (SISY), pp 187–192

Sarcevic P, Kincses Z, Pletl S (2015a) Comparison of different classifiers in movement recognition using WSN-based wrist-mounted sensors. IEEE Sensors Applications Symposium (SAS), pp 1–6

Sarcevic P, Schaffer L, Kincses Z, Pletl S (2015b) Hierarchical-distributed approach to movement classification using wrist-mounted wireless inertial and magnetic sensors. Infocommunications J 7:33–41

Suarez I, Jahn A, Anderson C, David K (2015) Improved activity recognition by using enriched acceleration data. In: Proceedings of the ACM International Joint Conference on Pervasive and Ubiquitous Computing (UbiComp), pp 1011–1015

Ugolotti R, Sassi F, Mordonini M, Cagnoni S (2013) Multi-sensor system for detection and classification of human activities. J Ambient Intell Human Comput 4:27–41. doi: 10.1007/s12652-011-0065-z

Varkey JP, Pompili D, Walls T (2012) Human motion recognition using a wireless sensor-based wearable system. Pers Ubiquitous Comput 16:897–910. doi: 10.1007/s00779-011-0455-4

Yang A, Jafari R, Sastry S, Bajcsy R (2009) Distributed recognition of human actions using wearable motion sensor networks. J Ambient Intell Smart Environ 1:103–115. doi: 10.3233/AIS-2009-0016

Zhu C, Sheng W (2011) Motion- and location-based online human daily activity recognition. Pervasive Mob Comput 7:256–269. doi: 10.1016/j.pmcj.2010.11.004